JOURNAL OF MATERIALS SCIENCE 30 (1995) 2849–2854

Al_2O_3 reinforced Al/Ni intermetallic matrix composite by reactive sintering

M. R. GHOMASHCHI
Department of Metallurgy, University of South Australia, The Levels, Adelaide, S.A. 5095, Australia

An aluminium–nickel reinforced Al_2O_3 particulate composite was fabricated by a powder metallurgy route, where 35 wt% aluminium and 30 wt% nickel powders were mixed with 35 wt% Al_2O_3 particles and compacted at 548 MPa. Sintering was carried out at 850 °C, where the synthesis reaction was sustained by the transient liquid phase resulting from the exothermic reaction associated with the formation of intermetallic compounds, i.e. reactive sintering. The resultant microstructure was studied using X-ray diffraction (XRD) and scanning electron microscopy coupled with energy dispersive spectroscopy (SEM–EDS). It was found that the initial distribution of individual constituent powders affect the outcome of the reactive sintering and that the inward diffusion of aluminium in nickel was responsible for nickel aluminide formation.

1. Introduction

Intermetallic compounds based on aluminium with nickel, iron or titanium offer new opportunities for developing superior/advanced structural alloys for applications as diversified as biomedical and aerospace–aircraft industries. Aluminides have the attractive characteristics of low density, high strength, good corrosion and oxidation resistance, non-strategic elements and relatively low cost. For a specific chemistry, these intermetallics exhibit the unique characteristics of improved strength with increasing temperature [1].

There are several techniques for synthesizing intermetallics, including conventional melting and solidification [2, 3], reactive sintering of constituent powders [4–8] and more recently, chemically induced shock consolidation of constituent powders [9], i.e. explosive bonding.

Reactive sintering, which is used in the present investigation, is quite effective and efficient in fabricating intermetallics. The synthesis reaction is sustained by a transient liquid phase resulting from exothermic reaction associated with the formation of the intermetallic compounds. There are several parameters that need to be understood, controlled and monitored closely to guarantee a sound sintered product. These include [4–8, 10–14]

1. system thermodynamics
2. mixture stoichiometry,
3. initial homogeneity,
4. particle morphology and size,
5. compacting pressure and green density,
6. compact size,
7. sintering atmosphere,
8. rate of heating,
9. soaking time and temperature,
10. percentage impurity,
11. green chemistry.

In addition to the above mentioned parameters, preheating and the temperature of compaction at the time of initiation may also be important in achieving denser and less distorted finished components.

If intermetallics are combined with ceramics, the resultant composite should be extremely attractive for applications where high strength and long creep life are required at high temperatures. At present, creep and oxidation resistance of nickel-based superalloys allow working temperatures up to 800–850 °C, while there is a strong desire to increase the working temperature to about 1000–1100 °C. Such improvement should offer less fuel consumption and faster speeds for jet engines, where these engineered intermetallic matrix composites are sought for use.

2. Experimental procedure

The aim of the present investigation was to study the fabrication of Al_2O_3 particulate reinforced aluminium–nickel alloys under different green chemistries, green compaction pressures, sintering times and temperatures, and sintering atmospheres. The present article reports initial results regarding the reaction at the sintering temperature.

A series of specimens with ring geometry, i.d. = 9.40 mm, o.d. = 19.15 mm and height = 7–8 mm, were prepared under a constant compaction pressure of 548 MPa using a 500 KN hydraulic press. The composition was 35 wt % Al_2O_3, 35 wt % aluminium and 30 wt % nickel, and 1 wt % zinc stearate was added as a lubricant; see Fig. 1 for particle size and distribution histograms. The tube furnace used in this

0022–2461

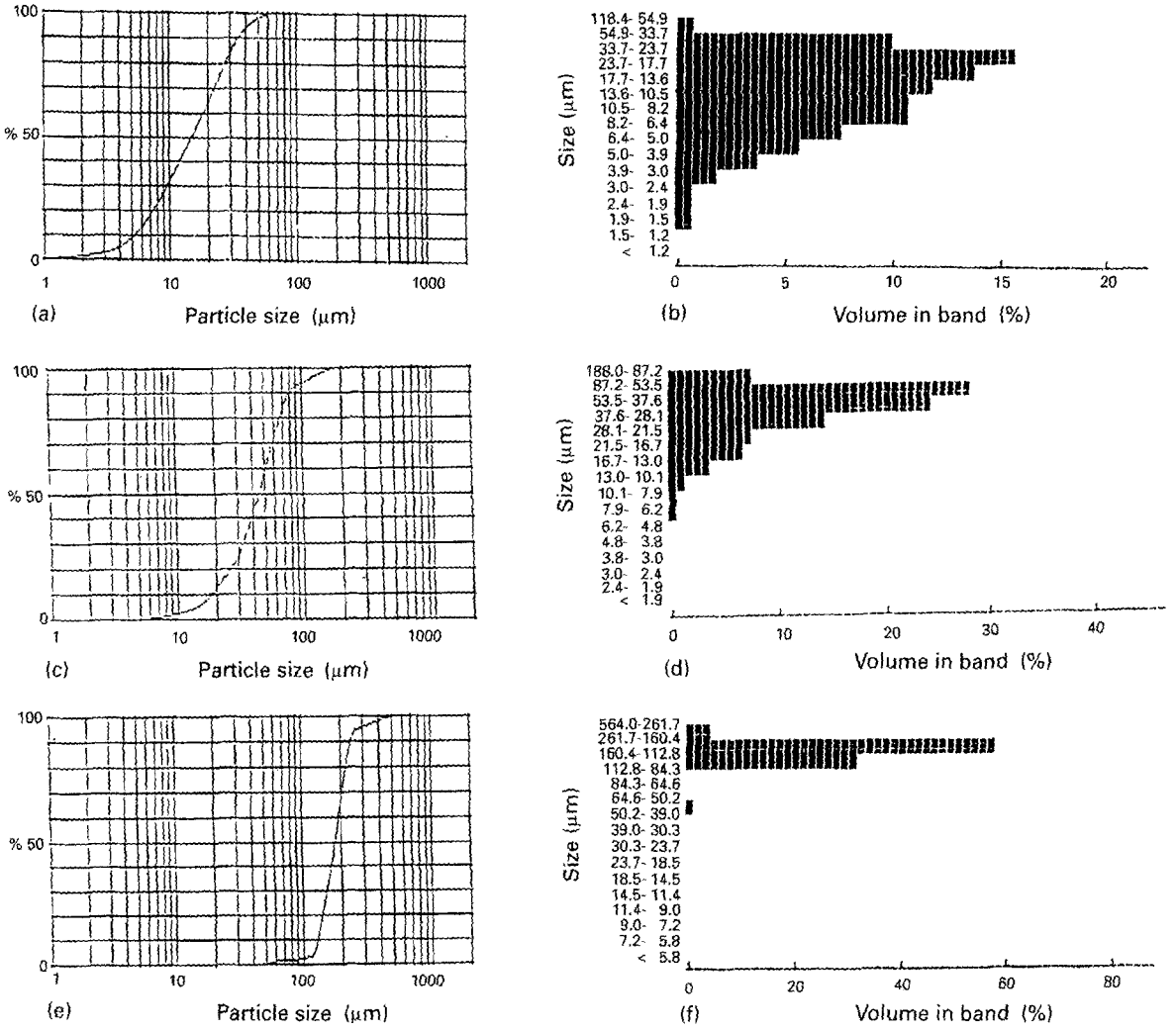

Figure 1 Cumulative and histogram size distribution graphs of particles used in this investigation. (a, b) nickel, (c, d) aluminium and (e, f) alumina.

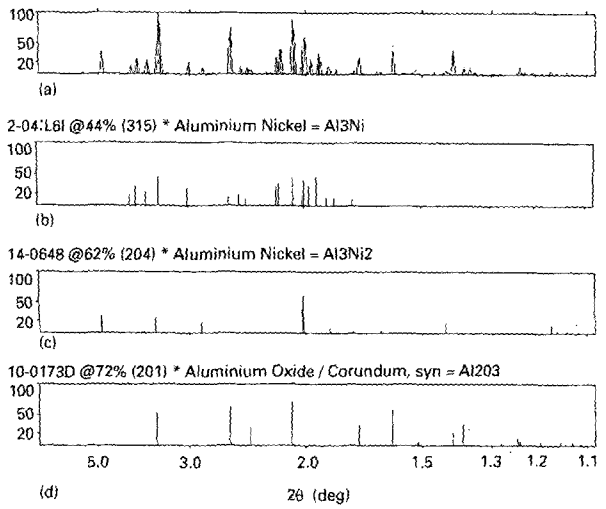

Figure 2 X-ray diffraction spectrum (a) of the reactive sintered alumina reinforced intermetallic matrix composite. Spikes for: (b) Al_3Ni, (c) Al_3Ni_2 and (d) Al_2O_3.

study, i.d. = 65 mm, was initially flushed with argon gas and then heated to 850 °C, while the specimens were held at the gas-end inlet within a stainless steel container, i.e. at temperature $T < 100$ °C. As the sintering temperature of 850 °C was achieved, the specimens were pulled into the furnace hot zone and held for 40 minutes before being quenched in water to room temperature immediately after withdrawal from the furnace hot zone. The rate of heating was rather fast and was estimated to be about 140–150 °C min^{-1}; the furnace temperature was stabilized to 850 °C within 6 min, after the specimen container was pulled into the furnace's hot zone.

All specimens were sectioned both longitudinally and transversally, polished and examined by optical and scanning electron microscopes. A small portion of the specimen was ground and prepared for XRD analysis using a Philips diffractometer. Energy dispersive X-ray microanalysis (EDX) was carried out on unetched specimens to identify the resultant phases. A Cambridge SEM/conventional Kevex and CamScan SEM/windowless detector were used.

3. Results

The matrix alloy, i.e. 35 wt % aluminium and 30 wt % nickel, on its own is equivalent to 54 wt % aluminium and 46 wt % nickel with a melting point around 1400 °C, and intermetallic phases of $NiAl_3$ and Ni_2Al_3 at room temperature, according to the aluminium–nickel phase diagram. The XRD analysis shown in Fig. 2 indicates the formation of $NiAl_3$, Ni_2Al_3 with Al_2O_3 reinforcement. The formation of these phases

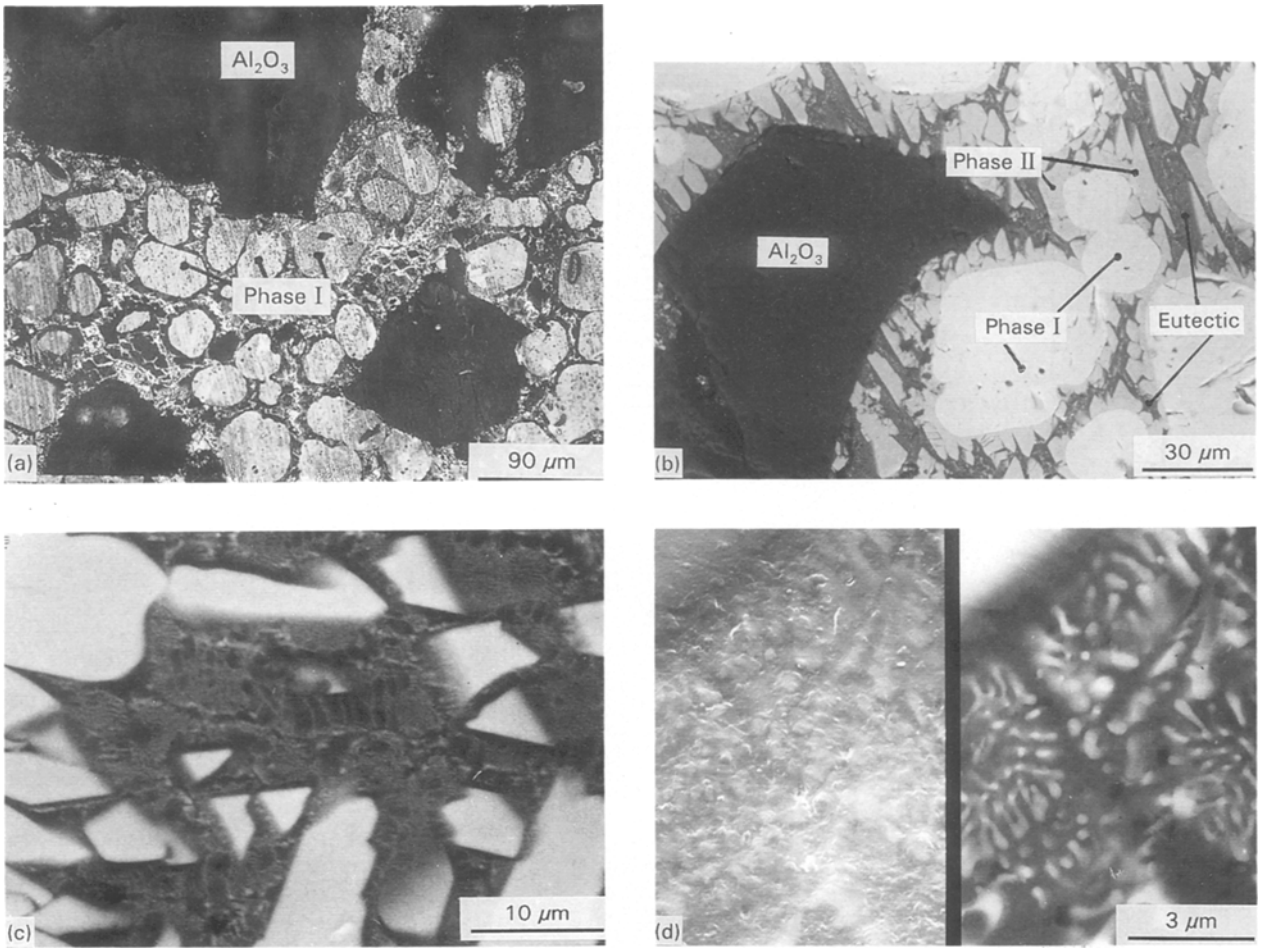

Figure 3 (a) Optical micrograph to show as-sintered specimen; Al_2O_3 = black regions. Backscattered electron images: (b) to show different phases formed during reactive sintering, (c) of the intercellular regions shown in Fig. 3b, (d) of the eutectic region shown in Fig. 3c.

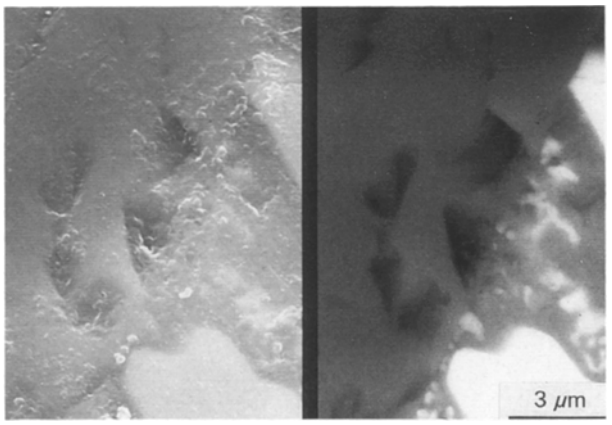

Figure 4 SEM micrograph showing the alumina–matrix interface.

confirms the success of reactive sintering at 850 °C. However, as shown in Fig. 3, the matrix is not simply a two phase mixture as predicted by the aluminium–nickel phase diagram. The optical micrograph in Fig. 3a shows black Al_2O_3 particulate, white rounded cells (phase I) and a complex mixture within the intercellular regions. Fig. 3b, which is a backscattered electron image, shows that the intercellular region comprises a grey phase (phase II) nucleated at the interface of phase I and a dark mixture. The dark mixture itself appears to have eutectic characteristics, as clearly shown in Fig. 3c and d. The Al_2O_3–matrix interface is shown in Fig. 4, where the majority of the interface area is covered with the so-called dark mixture illustrated in Fig. 3c and d. The EDX analysis of the phases detected in this study are presented in Fig. 5. The integrated area of the spectra was used to estimate the composition and thus the chemical formula, i.e. ZAF corrections were not applied. It was found that phase I, Fig. 3a, was stoichiometrically close to $Al_{12}Ni_5$, while phase II, Fig. 3b, was $Al_{12}Ni_3$. The eutectic type mixture, Fig. 3c and d, was comprised of highly enriched aluminium phases, where the black lamellae had slightly less nickel than the white phase in this mixture.

4. Discussion

There are three important points to be addressed with intermetallic matrix composite fabrication

1. The mechanism by which the aluminium and nickel particles were fused together produced an almost porosity free matrix.
2. What is the reinforcement role in this process?
3. What are the characteristics of the Al_2O_3–matrix interface?

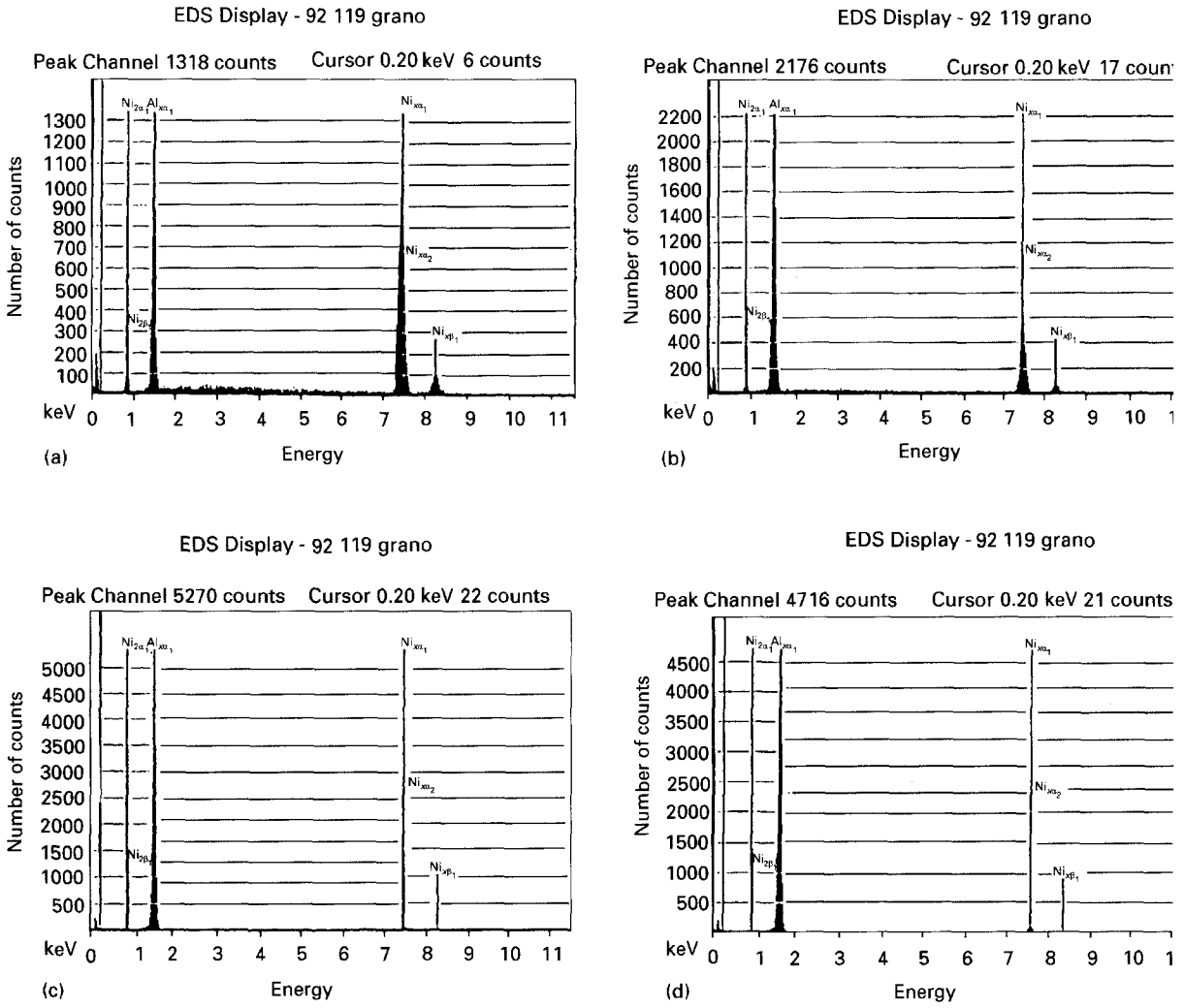

Figure 5 EDX spectra of the phases detected in the as-sintered specimen: (a) phase I, (b) phase II, (c) eutectic (black phase), (d) eutectic (white phase).

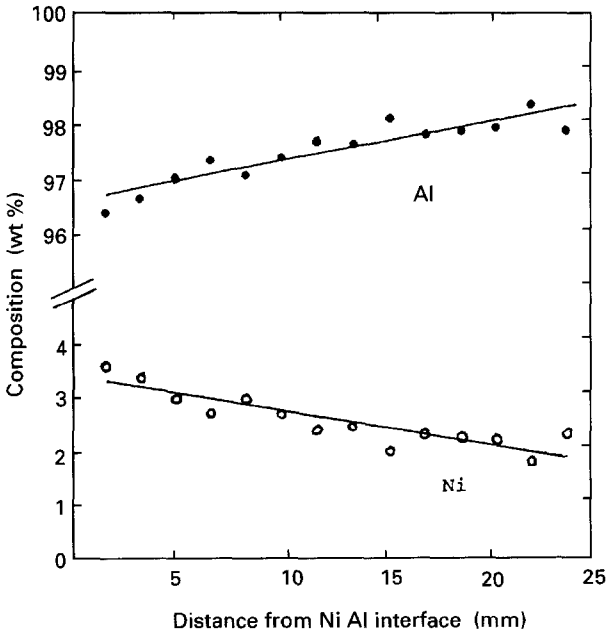

Figure 6 The distribution of nickel and aluminium from the interface within the nickel ball–liquid aluminium test.

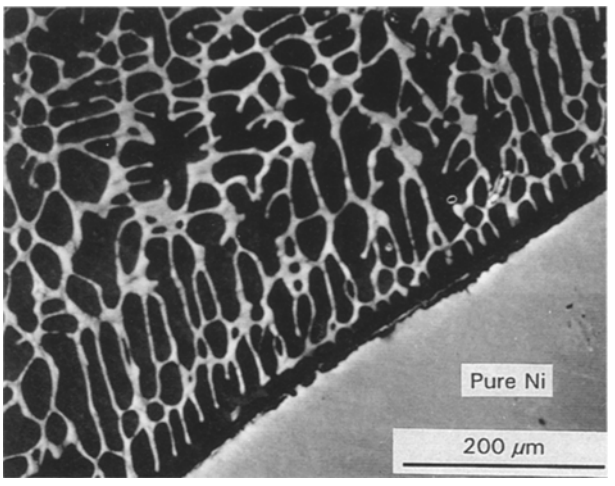

Figure 7 SEM micrograph to show the Al dendrites and Al–Ni eutectic.

In order to answer the first point, an attempt was made to simulate the interaction between the aluminium and nickel powders during sintering. A nickel ball, 10.49 mm diameter, was fully immersed in liquid aluminium (50–60 g) at 850 °C and held for 5 min at

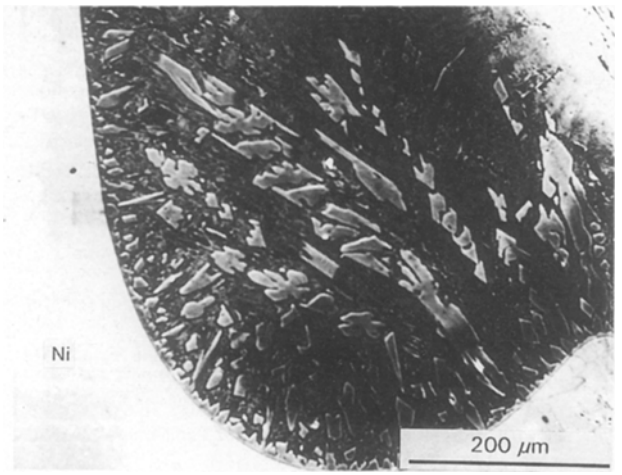

Figure 8 SEM micrograph showing the formation of an Ni-rich intermetallic phase in the Al-depleted region.

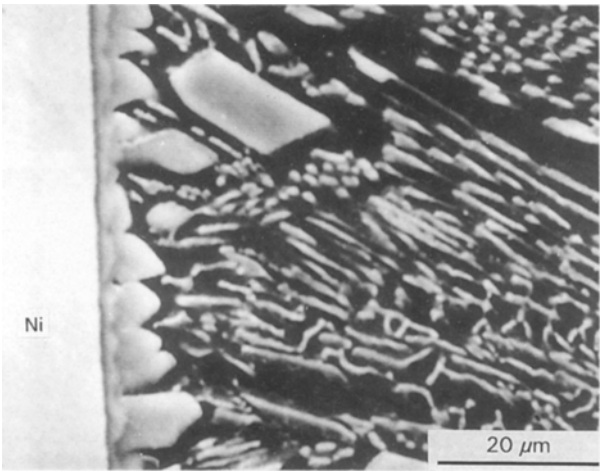

Figure 9 SEM micrographs showing the formation of Ni_3Al at the pure nickel interface.

this temperature. The metallic crucible containing the liquid aluminium and nickel ball was quenched in water to room temperature. The sample was sectioned and polished to achieve the largest possible nickel ball cross-section. The largest ball diameter containing pure nickel was measured and then used to estimate the rate of nickel consumption. It was found that approximately 0.004 $g\,s^{-1}$ nickel had diffused into liquid aluminium. Furthermore, nickel diffused at great distances from the initial nickel ball–aluminium liquid interface without any localized nickel enrichment. There was however, a continuous reduction of nickel concentration away from the nickel ball–aluminium interface, see Fig. 6. The formation of primarily aluminium dendrites and a eutectic mixture in Fig. 7 illustrates the rapid diffusion of nickel in liquid aluminium, which prevented local enrichment of nickel and thus the formation of primary intermetallic phases. However, if, somehow, the aluminium concentration diminishes, i.e. a small supply pool of aluminium as shown in Fig. 8, nickel-enriched intermetallic phases will form. High nickel content intermetallic phases, such as Ni_3Al, can only form by inward diffusion of liquid aluminium into nickel. The SEM micrograph in Fig. 9 shows the formation of Ni_3Al at the nickel–liquid aluminium interface. Thus;

1. High concentration nickel intermetallics do not form within liquid aluminium away from the initial aluminium–nickel interface. This is due to rapid diffusion of nickel in liquid aluminium, which prevents local enrichment of nickel. However, if nickel diffusion overwhelms aluminium, so that there is not enough liquid aluminium, then nickel-enriched intermetallics should form within the liquid aluminium away from the original aluminium–nickel interface.
2. Nickel enriched intermetallic phases may only form due to inward diffusion of liquid aluminium within solid nickel at the interface.

The results of the above mentioned tests were then employed to interpret the observed microstructure in Fig. 3.

Inter-diffusion of aluminium and nickel should not be considerable at temperatures below 659 °C, the melting point of aluminium; since the green compact was heated very rapidly to 850 °C. Therefore, the problem of solid state diffusion-formed intermetallics at nickel–aluminium particle interfaces should be very limited and cannot inhibit aluminium diffusion at the sintering temperature, as was suggested previously [5]. At the sintering temperature, the liquid aluminium tends to diffuse inwards into nickel, while nickel diffuses out in liquid aluminium. However, it appears that inward diffusion of aluminium is faster than outward diffusion of nickel. This is based on the formation of $Al_{12}Ni_5$ within the centre of nickel particles, while almost pure aluminium is present within inter-nickel particle regions. However, the XRD results are quite encouraging where Al_3Ni_2 and Al_3Ni have been detected. Therefore, the reactive sintering appears to have been quite successful. The presence of almost pure aluminium within intercellular regions, Fig. 3, may suggest an initial non-uniform distribution of aluminium and nickel powders, where not enough nickel particles were available to consume fully liquid aluminium at the sintering temperature.

As shown in Fig. 4, the Al_2O_3 reinforcement is used as nucleation sites for the phases formed within intercellular regions.

The Al_2O_3 particles appear to have bonded well with the matrix, regardless of the matrix composition at the interface. The integrity and mechanisms of failure of the Al_2O_3–matrix interface has been reported previously [3] for a conventionally cast Al_2O_3 reinforced aluminium–nickel intermetallic matrix composite, where in spite of good Al_2O_3–intermetallic bonding, i.e. adequate wetting, failure always occurred at the interface. For aluminium–Al_2O_3, however, failure was within the aluminium-rich phase, indicating effective bonding for aluminium and Al_2O_3.

5. Conclusions

1. Reactive sintering of aluminium, nickel and Al_2O_3 powders was achieved by heating the green compact at 850 °C.

2. XRD analysis confirmed the formation of Al_3Ni and Al_3Ni_2 as predicted by the aluminium–nickel phase diagram for the powder concentrations used in this investigation.

3. The inward diffusion of liquid aluminium in nickel was responsible for nickel aluminide formation.

4. The initial distribution of aluminium and nickel particles affected the outcome of the reactive sintering, where a non-uniform distribution resulted in excess aluminium within internickel particle regions.

Acknowledgements

The author is grateful to Len Green for part of the electron microscopy, Professor Ken Strafford for the provision of research facilities at the department, and Professor Polmear of Monash University for his constructive comments on the presentation of this article.

References

1. N. BALUK, J. BONNEVILLE, K. J. HEWKER, J. L. MARTIN, R. SCHÄUBLIN and P. SPÄTIG, *Mat. Sci and Eng.* **A164** (1993) 379–383.
2. M. R. GHOMASHCHI, Unpublished results, University of South Australia, 1991.
3. M. R. GHOMASHCHI, A. S. TAYABNAPIS and L. K. GREEN, Alumina particulate reinforced Aluminium-Nickel intermetallic matrix Composite "Advanced Composites 93", T. Chandra and A. K. Dhingra (eds) (JMS pub 1993) Wollongong, Australia, 15–19 February 1993 p 1385–1390.
4. K. S. HWANG and Y. U. LU, in International Conference "Advances in Powder Metallurgy", 20-23 May 1990, Pittsburg. *Metal Powder industry federation*, N. J., USA **2** pp. 133–144.
5. R. GERMAN, *ibid.*
6. J. C. MURRAY and R. M. GERMAN, *ibid.*
7. A. BOSE, B. H. RABIN and R. M. GERMAN, *Powder Met. Int.* **20** (1988) 25.
8. R. M. GERMAN and J. W. DUNLOP, *Metall. Trans.* **17A** (1986) 205.
9. D. M. BOWDEN, P. J. METSHTER, L. H. YU, M. A. MEYERS and N. N. THADHANI, J. of The Minerals, Metals & Materials Society (1988) 18.
10. V. M. MASLOV, I. P. BOROVINSKAYA and A. G. MERZHANOV, *Combust. Explos. Shock Waves* **12** (1976) 631.
11. Y. S. NAIBORODENKO and V. I. ITIN, *ibid.* **11** (1975) 293.
12. Z. A. MUNIR, *Ceram. Bull.* **67** (1988) 342.
13. V. I. ITIN, A. D. BRATCHIKOV and L. N. POSTNIKOVA, *Soviet Powder Met. Metal, Ceram.* **19** (1980) 315.
14. R. R. ODDONE and R. M. GERMAN, *Adv. Powder Met.* **3** (1989) 475.

Received 11 April
and accepted 2 August 1994